Journal Name

COMMUNICATION

Liquid phase exfoliation of carbonate-intercalated layered double hydroxides

Received 00th January 20xx,
Accepted 00th January 20xx

DOI: 10.1039/x0xx00000x

www.rsc.org/

Jose A. Carrasco,[a,‡] Andrew Harvey,[b,‡] Damien Hanlon,[b] Vicent Lloret,[c] Dave McAteer,[b] Roger Sanchis-Gual,[a] Andreas Hirsch,[c] Frank Hauke,[c] Gonzalo Abellán,[a,c,*] Jonathan N. Coleman,[b,*] Eugenio Coronado.[a]

Direct exfoliation of a carbonate layered double hydroxide (LDHs) has been achieved by using a novel horn-probe sonic tip, avoiding the development of time-consuming anion-exchange reactions. Most suitable solvents were chosen based on the Hildebrand solubility parameters and the thickness of the exfoliated nanosheets confirmed unambiguously the successful delamination.

Layered double hydroxides (LDHs) are a class of ionic layered materials which display a brucite-like structure with the general formula $[M^{II}_{1-x}M^{III}_{x}(OH)_2]^{x+}(A^{n-})_{x/n}\cdot mH_2O$.[1,2] The main structure of a LDH highlights the cationic hydroxide sheets and the presence of the interlayer anions compensating the excess of positive charge (**SI1**, **ESI**†). In addition to that, one can find solvent molecules surrounding the structure. A key aspect of these materials is their ability to replace their interlayer anion thanks to anion exchange reactions. Hence, the rational choice of the metals and the interlayer anion can tune the final properties of the material, and LDHs are reported to exhibit a wide range of applications in diverse fields such as catalysis, anion exchange, sensing, magnetism or energy storage, among others.[3–5] One of their most interesting features is their possibility to be exfoliated into 2D nanosheets, acting as macromolecular building blocks for the synthesis of more complex architectures while they retain the fundamental properties of the pristine bulk precursors such as the 2D magnetism or redox behaviour.[5] In this context, the ionic nature of the LDHs hinders the exfoliation procedure in stark contrast with other 2D van der Waals materials,[6] and time-consuming anion exchange reactions are mandatory to reduce the strength of the electrostatic interactions between the cationic layers and the interlayer anion. In a typical synthesis, LDHs are obtained with carbonate (CO_3^{2-}) in the interlayer space due to the higher affinity with respect to other anions, and therefore the direct exfoliation of a CO_3^{2-}–LDH is believed to be almost impossible.[7] To overcome this inconvenience, other monovalent anions such as nitrate, chloride or anionic surfactants are introduced in the LDH structure by replacing the carbonate moiety and weakening the electrostatic interactions.[8–10] In addition to that, formamide (which is highly toxic) stands out as the main solvent to carry out the exfoliation of LDHs, thanks to the ability to produce a swollen phase between the hydroxide sheets prior to the delamination.[11] It is suggested that the driving force for the swelling of the LDH may be ascribed with the hydrogen bonding between the electronegative elements (O and N) of the solvent and the hydroxide sheets, allowing its penetration into the gallery space and subsequent exfoliation.[12] Nevertheless, the high boiling point of formamide (210 °C) makes the evaporation difficult and therefore the processability of the nanosheets after the deposition on different substrates. Thus, alternative approaches are of utmost importance.

Here we report for the very first time the direct exfoliation of a CO_3^{2-}–LDH using liquid phase exfoliation *via* ultrasonic tip. This method has reported successful results in the exfoliation

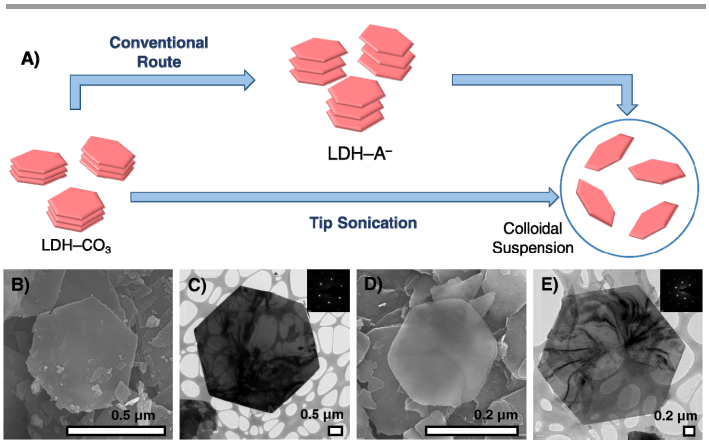

Fig. 1 (A) Scheme comparing the conventional exfoliation route and the tip sonication approach for LDHs. FESEM images of (A) CoAl–CO_3 and (D) CoAl–DS. TEM images of (C) CoAl–CO_3 and (E) CoAl–DS highlighting in the inset the crystallinity of the material *via* SAED patterns.

[a] *Instituto de Ciencia Molecular, Universitat de València, Catedrático José Beltrán 2,46980, Paterna, Spain.*
[b] *School of Physics and CRANN & AMBER Research Centers, Trinity College Dublin, Dublin 2, Ireland.*
[c] *Department of Chemistry and Pharmacy, University Erlangen-Nürnberg, Henkestr. 42, 91054 Erlangen (Germany).*
† Footnotes relating to the title and/or authors should appear here.
Electronic Supplementary Information (ESI) available. See DOI: 10.1039/x0xx00000x
‡ JAC and AH contributed equally to this work.

of layered inorganic materials such as transition metal dichalcogenides,[13] simple hydroxides,[14] black phosphorus[15] or antimonene,[16] to name a few.[17,18] The use of tip sonication is novel on the LDH field, in stark contrast with the most typical bath sonication approach.[10] A scheme describing the conventional and the novel tip sonication route for the LDHs can be found in **Fig. 1A**. The results were compared with the exfoliation of a dodecyl sulphate–LDH (DS–LDH), obtained after successive anion exchange reactions on the carbonate sample. Furthermore, different solvents were tested based on their Hildebrand solubility parameters to explore more suitable alternatives to formamide.

To start with, highly crystalline CoAl–CO_3 sample was synthesized following the method described by Liu *et al.,*[7] (see **SI2** and **SI3**, **ESI†** for additional experimental details) using urea as an ammonia-releasing reagent to achieve a well-defined hexagonal morphology.[3,19,20] The dodecyl-intercalated CoAl–DS sample was obtained after two successive anion exchange reactions, first to nitrate using the acid-salt approach[21] and afterwards to dodecyl sulphate. The synthesis of the LDH phase was confirmed by X-ray powder diffraction (XRPD) (**SI4**, **ESI†**), exhibiting the main basal reflections for hydrotalcite-like materials (JCPDS 22-700).[20,22] The main (003) peak is related with the basal space of the LDH material, therefore shifting towards lower 2-Θ values as the length of the intercalated anion increases. The basal spaces for the CoAl–CO_3 and CoAl–DS samples are found to be 7.6 and 26.7 Å, respectively.[3] The nature of the interlayer species was also confirmed *via* attenuated total reflectance Fourier transform infrared (ATR-FTIR) spectroscopy (**SI4**, **ESI†**). The bands observed at *ca.* 3400 and 1600 cm^{-1} are related to the O–H bonding from the hydroxyl groups and the H_2O molecules, respectively. The CoAl–CO_3 also exhibits a strong peak at *ca.* 1350 cm^{-1}, indicative of the v_3 stretching mode of CO_3^{2-} as the interlayer anion.[20,23] Regarding the CoAl–DS, the most important peaks are the ones found at *ca.* 2917 and 2845 cm^{-1}, related with the C–H stretching. These bands are assigned to the presence of the surfactant and indicative of the successful intercalation of the dodecyl sulphate.[3,24] According to the model proposed by Lagaly, we can expect a bilayer arrangement of the surfactant molecules between the hydroxide sheets with tilt angles between *ca.* 9–24°.[25] Thermogravimetric analysis (TGA) (**SI4**, **ESI†**) also depicted the typical profile for the LDHs, with an initial weight loss in the 25–220 °C range, ascribed to the removal of adsorbed and interlayer H_2O molecules (solvation molecules) and a second weight loss in the 220–600 °C range, related with the dehydroxilation of the layers and the decomposition of the interlayer anion.[20,26] When larger molecules such as the dodecyl sulphate are introduced in the interlayer space of the LDH, an increase in the final weight loss can be observed (from 70% to 40% after exchanging CO_3^{2-} by DS^-) .[3]

The morphology of the bulk material was also imaged *via* electron microscopy (FESEM and TEM, **Fig. 1B–1E**). Both samples exhibited a well-defined hexagonal morphology as expected for –Al^{3+} LDHs synthesized in presence of ammonium releasing reagents (ARR) such as urea.[7] This hexagonal morphology is conserved after the anion exchange reaction of DS^-, and the average lateral size of CoAl–CO_3 and CoAl–DS samples was found to be *ca.* 5.0 µm in both cases (see histograms in **SI5**, **ESI†**). In addition to that, selected area electron diffraction (SAED) pattern confirmed the high crystalline quality of the LDHs, in good agreement with that observed in the XRPD.[27] Additional FESEM images can be found in **SI6**, **ESI†**.

The exfoliation of the materials was carried out following the methodology reported by some of us for other layered inorganic materials, consisting in the use of a tip sonication approach (see **SI3**, **ESI†** for additional experimental details).[14–17] In nanomaterials, the stabilization is achieved when the solubility parameters between solvent and solute match.[28] Due to this, not all solvents lead to stable dispersions in function of the solute. Therefore, the understanding of the solubility parameters developed by Hildebrand and Hansen becomes crucial to comprehend the chemistry that relies on the exfoliation into stable nanosheet dispersions.[17,29] For the first time, a complete solubility study on LDHs has been carried out using a total amount of 19 solvents based on their Hildebrand parameters. The complete solvent list can be found in **SI7**, **ESI†**. Both CoAl–CO_3 and CoAl–DS were dispersed in each solvent as described in **SI3**, **ESI†** and the extinction spectra were measured using a UV-vis spectrometer. Extinction spectra become crucial for the nanomaterial dispersions since it takes into account the contribution from light scattering, non-trivial for the case of 2D nanosheets.[30] **Fig. 2A–2B** depicts the solubility diagrams for CoAl–CO_3 and CoAl–DS based on the value obtained at 450 nm. Extinction spectra in the 350–500 nm region can be found in **Fig. 2C–2D**. After the fitting of the results to a Gaussian function,[15,31] as demonstrated with other materials exfoliated using this method, we found the best results for the N-Cyclohexyl-2-

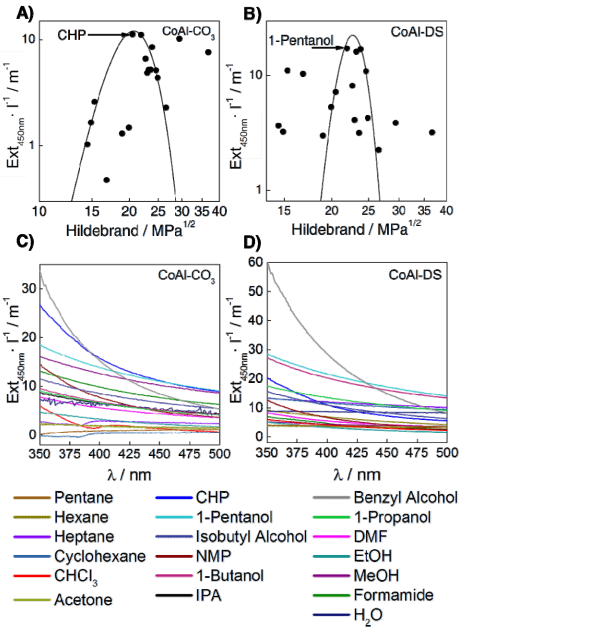

Fig. 2 Solubility diagrams of (A) CoAl–CO_3 and (B) CoAl–DS samples in a wide variety of solvents. Extinction spectra in the 350–500 nm region of (C) CoAl–CO_3 and (D) CoAl–DS. Solvent list table and the corresponding solubility parameters can be found in SI8, ESI†.

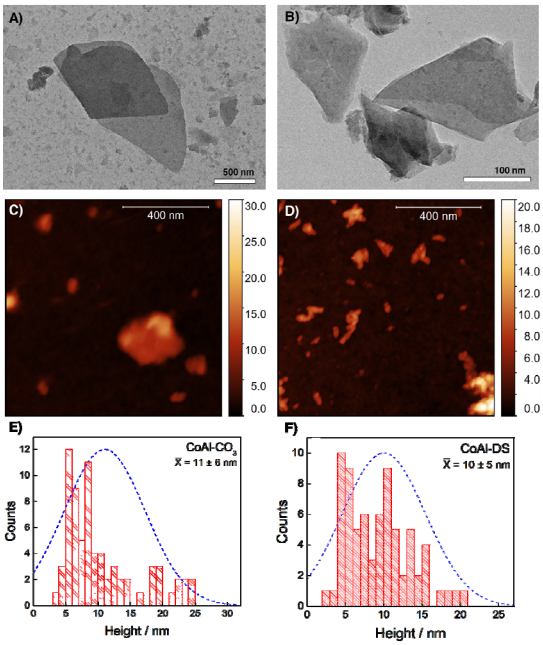

Fig. 3 TEM and AFM images of the (A and C) CoAl–CO_3 and (B and D) CoAl–DS nanosheets in CHP and 1-Pentanol, respectively. Histograms with the measured thickness of 75 nanosheets for (E) CoAl–CO_3 and (F) CoAl–DS deposited nanosheets.

pyrrolidone (CHP) and the 1-Pentanol for the CoAl–CO_3 and CoAl–DS samples, respectively, with Hildebrand parameters in the range of *ca.* 20.5–23 $M{\cdot}Pa^{0.5}$, similar to other layered materials.[17] In addition, it is observed that some solvents exhibit higher concentration (ext/l) values than the observed for the typical formamide. For the CoAl–CO_3 sample, formamide displays a concentration (ext/l) value of *ca.* 7.6 m^{-1}, while solvents such as CHP, 1-Pentanol, benzyl alcohol and MeOH surpass it with values of 11.2, 11.1, 8.5 and 10.2 m^{-1}, respectively. Regarding the CoAl–DS material, formamide depicts a concentration (ext/l) value of *ca.* 3.2 m^{-1}, easily surpassed by most of the solvents employed (such as 1-Pentanol, 1-Butanol, benzyl alcohol or 1-Propanol exhibiting values of 17.2, 16.1, 17.0 and 10.9 m^{-1}, respectively). Nanosheet dispersions were characterized *via* TEM and atomic force microscopy (AFM). TEM images exhibited lateral sizes of several hundreds of nanometers for both samples, pointing out the fracture of the crystals after the sonication procedure (**Fig. 3A–3B**). Additional TEM images can be found **SI8** and **SI9**, **ESI†**. The stability of the CoAl–CO_3 suspension was analysed *via* UV-Vis, dynamic light scattering (DLS) and Tyndall effect, exhibiting no reaggregation processes and an average size of 430 nm (**SI10**, **ESI†**). On the other hand, the dispersions were spin coated on SiO_2 substrates at 5000 r.p.m. and the thickness of the nanosheets was measured using AFM (**Fig. 3C–3D**). Histograms for both samples are depicted in **Fig. 3E–3F**, exhibiting an average thickness of *ca.* 11 and 10 nm for CoAl–CO_3 and CoAl–DS, respectively. Both results are statistically comparable and one order of magnitude lower than the thickness of the bulk materials (**SI11**, **ESI†**), hence achieving for the first time the direct exfoliation of a CO_3^{2-}–LDH by using any exfoliation technique. Since an ideal LDH mono-layer is experimentally in the range of 0.6–0.8 nm in thickness,[8] here we report the delamination into an average few-layer system. On top of that, thicknesses below 10 nm (especially in the low range 3–6 nm) can be easily found according to the histogram, hence paving the way for the isolation of those nanosheets *via* size selection in cascade centrifugation.[13] Height profiles for some individual nanosheets with a discussion on the lower limit of the thickness of nanosheets and the homogeneity after the exfoliation are depicted in **SI12** and **SI13**, **ESI†**. The attempt to exfoliate CoAl–CO_3 using the conventional bath sonication approach leads to the unsuccessful exfoliation, as expected. This control experiment including the complete characterization can be found in **SI14**, **ESI†**.

In addition, to demonstrate the usefulness of this approach we have explored the exfoliation of LDHs having different lateral dimensions and chemical composition. More concretely, we successfully exfoliated a nanometric (*ca*. 400 nm) CoAl–CO_3 prepared using a traditional coprecipitation approach[26], and a hexagonal NiFe–CO_3 synthesized using the ARR route (**SI15** and **SI16**, **ESI†**).[8,20] In order to illustrate the potential of this new direct exfoliation route of LDHs *via* tip sonication, electrochemical measurements were tested on the CoAl–CO_3 exfoliated nanosheets (**SI15** and **SI16**, **ESI†**) and compared with the bulk materials as a catalyst for the oxygen evolution reaction (OER).[32,33] Linear sweep voltammetry (LSV) was performed in order to evaluate the oxygen evolution activity in 1 M NaOH at 1 $mV{\cdot}s^{-1}$ scan rate, obtaining the polarisation curves shown in **Fig. 4A**. An improvement in the OER performance is observed for the directly exfoliated CoAl–CO_3 nanosheets compared with the respectively bulk LDHs, decreasing significantly the overpotential required for a current density of 10 $mA{\cdot}cm^{-2}$ in *ca.* 30 mV, and the Tafel slope in *ca.* 3 $mV{\cdot}dec^{-1}$.[10] These results are in good agreement with those reported for previously intercalated–LDHs and are indicative of the delamination of the material, as seen in **Fig. 3E**.[10] It is important to notice the larger OER activity in

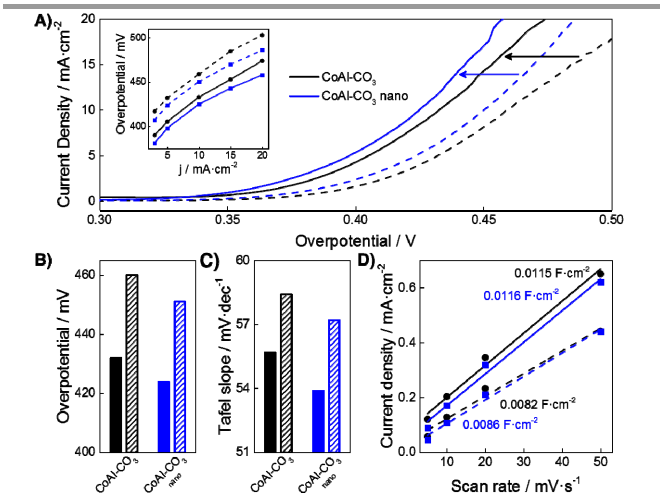

Fig. 4 Electrochemical performance of the CoAl–CO_3 samples (exfoliated LDHs in solid lines and bulk LDHs in dash lines). Inset: Overpotential measured at different current densities. (A) Linear sweep voltammetry performed at 1 $mV{\cdot}s^{-1}$ in 1 M NaOH. (B) Overpotentials required for j = 10 $mA{\cdot}cm^{-2}$ and (C) Tafel slopes calculated from the LSV data. (D) Electrochemical Surface Area calculated from CVs performed in a non-faradaic region at different scan rates.

nanosized LDHs, displaying lower overpotentials as well as Tafel slopes values. The enhancement in the OER is due to the increase in both the specific surface area and the number of active edge sites.[10] Along this front, Electrochemical Surface Area (ECSA) of the exfoliated and the bulk samples were analysed by obtaining the double layer capacitance (**Fig. 4D**). This value was calculated from cyclic voltammetry curves measured in a non-Faradaic region at different scan rates. The slopes of the fitted plots correspond to the double layer capacitance. The exfoliated samples have a value *ca.* 1.4 higher than the bulk materials, confirming the successful exfoliation regardless of the size of the LDH used (see **Fig. 4D**). Last but not least, this tip exfoliation method was also tested on NiFe-CO_3 LDH exhibiting higher improvement reducing the overpotentials and Tafel slopes values (**SI15** and **SI16**, **ESI**†).

In summary, we report for the first time the direct exfoliation of a CO_3^{2-}–LDH into few-layer nanosheets using a tip sonication methodology. The results were statistically equivalent with the observed for the delamination of a DS–LDH, with an average thickness of *ca.* 10 nm in both materials and the presence of a high number of nanosheets in the 3–6 nm range. A novel and complete solubility study on the LDH field based on the Hildebrand parameters was carried out for a wide variety of solvents, measuring their extinction spectra in an integrating sphere. Best solvents were found in the 20.5–23 $M \cdot Pa^{0.5}$, in good agreement with the expected for other inorganic layered materials. These results open a new approach in the field of the exfoliation of LDH and pave the way for their processability.

This work was partially supported by the European Research Council (ERC Starting Grant 2D-PnictoChem 804110 to G.A.). The research leading to these results was partially funded by the European Union Seventh Framework Programme under grant agreement No. 785219 and 604391, Graphene Flagship. J. N. C. thanks the Science Foundation Ireland (SFI) funded centre AMBER (SFI/12/RC/2278). G.A. has received financial support through the Postdoctoral Junior Leader Fellowship Programme from "la Caixa" Banking Foundation. G.A. thanks support by the Deutsche Forschungsgemeinschaft (DFG; FLAG-ERA AB694/2-1), and the Generalitat Valenciana (SEJI/2018/034 grant). A.H. thank the SFB 953 "Synthetic Carbon Allotropes "funded by the DFG for support and the Cluster of Excellence "Engineering of Advanced Materials". This work was supported by the Spanish MINECO and Excellence Unit María de Maetzu (MDM-2015-0538).

Conflicts of interest

There are no conflicts to declare.

Notes and references

1 C. Forano, T. Hibino, F. Leroux and C. Taviot-Guého, in *Developments in Clay Science*, Elsevier, 2006, vol. 1, pp. 1021–1095.
2 G. Abellán, C. Martí-Gastaldo, A. Ribera and E. Coronado, *Acc. Chem. Res.*, 2015, **48**, 1601–1611.
3 J. A. Carrasco, S. Cardona-Serra, J. M. Clemente-Juan, A. Gaita-Ariño, G. Abellán and E. Coronado, *Inorg. Chem.*, 2018, **57**, 2013–2022.
4 M. Xu and M. Wei, *Adv. Funct. Mater.*, 2018, 1802943.
5 Q. Wang and D. O'Hare, *Chem. Rev.*, 2012, **112**, 4124–4155.
6 K. S. Novoselov, A. Mishchenko, A. Carvalho and A. H. Castro Neto, *Science*, 2016, **353**, aac9439.
7 Z. Liu, R. Ma, M. Osada, N. Iyi, Y. Ebina, K. Takada and T. Sasaki, *J. Am. Chem. Soc.*, 2006, **128**, 4872–4880.
8 G. Abellán, E. Coronado, C. Martí-Gastaldo, E. Pinilla-Cienfuegos and A. Ribera, *J. Mater. Chem.*, 2010, **20**, 7451–7455.
9 N. Mao, C. H. Zhou, D. S. Tong, W. H. Yu and C. X. Cynthia Lin, *Appl. Clay Sci.*, 2017, **144**, 60–78.
10 F. Song and X. Hu, *Nat. Commun.*, 2014, **5**, 4477, 1–9.
11 R. Ma, Z. Liu, L. Li, N. Iyi and T. Sasaki, *J. Mater. Chem.*, 2006, **16**, 3809–3813.
12 T. Hibino, *Chem. Mater.*, 2004, **16**, 5482–5488.
13 C. Backes, B. M. Szydłowska, A. Harvey, S. Yuan, V. Vega-Mayoral, B. R. Davies, P. Zhao, D. Hanlon, E. J. G. Santos, M. I. Katsnelson, W. J. Blau, C. Gadermaier and J. N. Coleman, *ACS Nano*, 2016, **10**, 1589–1601.
14 A. A. S. Rovetta, M. P. Browne, A. Harvey, I. J. Godwin, J. N. Coleman and M. E. G. Lyons, *Nanotechnology*, 2017, **28**, 375401.
15 D. Hanlon, C. Backes, E. Doherty, C. S. Cucinotta, N. C. Berner, C. Boland, K. Lee, A. Harvey, P. Lynch, Z. Gholamvand, S. Zhang, K. Wang, G. Moynihan, A. Pokle, Q. M. Ramasse, N. McEvoy, W. J. Blau, J. Wang, G. Abellan, F. Hauke, A. Hirsch, S. Sanvito, D. D. O'Regan, G. S. Duesberg, V. Nicolosi and J. N. Coleman, *Nat. Commun.*, 2015, **6**, 8563.
16 C. Gibaja, D. Rodriguez-San-Miguel, P. Ares, J. Gómez-Herrero, M. Varela, R. Gillen, J. Maultzsch, F. Hauke, A. Hirsch, G. Abellán and F. Zamora, *Angew. Chem. Int. Ed.*, 2016, **55**, 14345–14349.
17 C. Backes, T. M. Higgins, A. Kelly, C. Boland, A. Harvey, D. Hanlon and J. N. Coleman, *Chem. Mater.*, 2017, **29**, 243–255.
18 V. Nicolosi, M. Chhowalla, M. G. Kanatzidis, M. S. Strano and J. N. Coleman, *Science*, 2013, **340**, 1226419–1226419.
19 G. Abellán, J. L. Jordá, P. Atienzar, M. Varela, M. Jaafar, J. Gómez-Herrero, F. Zamora, A. Ribera, H. García and E. Coronado, *Chem Sci*, 2015, **6**, 1949–1958.
20 J. A. Carrasco, G. Abellán and E. Coronado, *J. Mater. Chem. C*, 2018, **6**, 1187–1198.
21 N. Iyi, T. Matsumoto, Y. Kaneko and K. Kitamura, *Chem. Mater.*, 2004, **16**, 2926–2932.
22 L.-J. Zhou, X. Huang, H. Chen, P. Jin, G.-D. Li and X. Zou, *Dalton Trans*, 2015, **44**, 11592–11600.
23 T. Xiao, Y. Tang, Z. Jia, D. Li, X. Hu, B. Li and L. Luo, *Nanotechnology*, 2009, **20**, 475603.
24 R. B. Viana, A. B. F. da Silva and A. S. Pimentel, *Adv. Phys. Chem.*, 2012, **2012**, 1–14.
25 M. Meyn, K. Beneke and G. Lagaly, *Inorg. Chem.*, 1993, **32**, 1209–1215.
26 J. A. Carrasco, J. Romero, M. Varela, F. Hauke, G. Abellán, A. Hirsch and E. Coronado, *Inorg Chem Front*, 2016, **3**, 478–487.
27 C. Hobbs, S. Jaskaniec, E. K. McCarthy, C. Downing, K. Opelt, K. Güth, A. Shmeliov, M. C. D. Mourad, K. Mandel and V. Nicolosi, *Npj 2D Mater. Appl.*, 2018, **2**, 4.
28 P. May, U. Khan, J. M. Hughes and J. N. Coleman, *J. Phys. Chem. C*, 2012, **116**, 11393–11400.
29 J. M. Hughes, D. Aherne and J. N. Coleman, *J. Appl. Polym. Sci.*, 2013, **127**, 4483–4491.
30 A. A. Kokhanovsky, Ed., *Light scattering reviews: single and multiple light scattering*, Springer ; Published in association with Praxis, Berlin ; New York : Chichester, 2006.
31 A. Harvey, C. Backes, Z. Gholamvand, D. Hanlon, D. McAteer, H. C. Nerl, E. McGuire, A. Seral-Ascaso, Q. M. Ramasse, N. McEvoy, S. Winters, N. C. Berner, D. McCloskey, J. F. Donegan, G. S. Duesberg, V. Nicolosi and J. N. Coleman, *Chem. Mater.*, 2015, **27**, 3483–3493.
32 Y.-C. Liu, J. A. Koza and J. A. Switzer, *Electrochimica Acta*, 2014, **140**, 359–365.
33 D. McAteer, I. J. Godwin, Z. Ling, A. Harvey, L. He, C. S. Boland, V. Vega-Mayoral, B. Szydłowska, A. A. Rovetta, C. Backes, J. B. Boland, X. Chen, M. E. G. Lyons and J. N. Coleman, *Adv. Energy Mater.*, 2018, **8**, 1702965.

